UDC 629 . 11 . 011 : 669 . 14 . 018 . 26 : 621 . 791 . 763 . 1

Technical Report

Assembly Technology of Welding and Joining for Ultra-high Strength Steel Sheets for Automobiles —Spot Welding—

Seiji FURUSAKO*
Tasuku ZENIYA
Tohru OKADA
Hiroki FUJIMOTO
Sho MATSUI
Chisato WAKABAYASHI
Naoaki SHIMADA

Abstract

Ever higher collision safety and fuel efficiency are required for automobiles. In response to this requirement, the application of high strength steel sheets is expanding, and simultaneously, further strengthening of high strength steel sheets is desired. In order to expand the application of such high strength steel sheets, it is essential to ensure their weld strength reliability. Therefore, the results of research that examined improvement of the welding strength of high strength steel sheets, mainly resistance spot welding, are summarized. Peel strength of the resistance spot welded joint is governed by toughness of the weld. Reducing the solidification segregation at the weld and tempering the martensite generated in the weld are effective for improving the peel strength. Post-heat to realize the martensitic tempering in the resistance spot welding, the use of arc-spot welding and the combined use of spot welding and laser welding are also described as methods to suppress the fracture of the weld and improve the bending property of hat-shaped components. From the viewpoint of structure and welding techniques, a new patchwork tailored blanking technique, in which spot welds are placed on the ridgeline (bending R portion) to improve the bending characteristics of a component, is also described. In addition, examples in which LME (Liquid Metal Embrittlement) cracks generated in spot welds are prevented by devising electrode shapes and the development of dissimilar material joining technology utilizing EJOWELD® are also presented.

1. Introduction

In order to meet both the strengthened requirements of automotive collision safety regulations and needs to reduce weight for the purpose of fuel consumption improvement, the application of high strength steel sheets to car bodies is rapidly growing.[1, 2] As such steel sheets used for car bodies are press-formed into products, excellent press-formability as well as high strength are required. Strength and formability are mutually exclusive, so in order to make both characteristics compatible, the amounts of additives such as C and Mn need to be adjusted, and control of the microstructure in the production process is also required. To improve the shape fixability and reduce the pressing force in the press-forming of high strength steel sheets, the use of hot-stamping steel sheets is also promoted. In such steel sheets, in order to secure the strength and the hardenability, C and Mn are added. However, such elements generally deteriorate the weldability. For example, in steel sheets with strength ex-

* Senior Researcher, Dr.Eng., Welding & Joining Research Lab., Steel Research Laboratories
20-1 Shintomi, Futtsu City, Chiba Pref. 293-8511

ceeding 780 MPa, the cross tension strength of a joint joined by the resistance spot weld (RS weld) (hereinafter collectively referred to as "spot weld") deteriorates as the steel sheet strength increases.[3, 4] As the fracture of the weld destabilizes the crashworthiness of car bodies, various weld-strength improving measures have been proposed.

This report describes the improvement of current applications as a means to improve the spot-welded joint strength of high strength steel sheets[5] and presents the results of the study. This study aimed to improve the performance of a modelled component by using high strength steel sheets, wherein the weld fracture was prevented by developing the welding process. Specifically the effects of the following measures on preventing the weld fracture are described: improvement of the current applications of spot welding, utilization of arc spot welding (hereinafter referred to as "AS welding")[6, 7] and the combined use of spot welding and laser welding. Furthermore, this report presents the result of the study conducted to prevent the liquid metal embrittlement (LME) crack generated in the spot welding by changing the design of the electrode tip front, and the development of the dissimilar material joining technique by applying EJOWELD®.

2. Improvement of Spot-welded Joint Strength by Post-heat Application

Enhancement of the strength of automotive high strength steel sheets is in progress. To realize this, elements such as C, Si and Mn are added to the steel sheets, any of which enhance the hardenability of the steel sheets. In addition, in spot welding, as the steel sheets are pressed by water-cooled copper electrodes, and the welding heat is released thereby, the cooling rate is very high. Accordingly, in the high strength steel sheets containing carbon of equal to or higher than 0.1 mass%, the weld metal formed by spot welding and its neighboring heat affected zone (HAZ) are quenched (a martensitic microstructure is formed). The toughness of the quenched and hardened microstructure is low, which causes the low spot-welded joint strength of the high strength steel sheets.

Figure 1 shows the relationship between steel sheet strength and spot-welded joint strength. The tensile shear strength (TSS) increases along with the increase of the steel sheet strength. This is because TSS is governed mainly by the strength (hardness) of the weld. However, in steel sheet strength that exceeds 780 MPa, the cross tension strength (CTS) decreases as the steel sheet strength increases. In the CTS test, as a nugget is considered to be of a shape surrounded by cracks on all its sides, and as the stress is concentrated at the edge of the nugget,[8] the strength is considered to be governed by the toughness of the weld.[9] Enlarging the nugget diameter is considered to be a basic means to improve the spot-welded joint strength. However, the nugget diameter is restricted by the electrode tip diameter and/or the flange width for welding. Therefore, the method of improving the joint strength by developing the current applications is hereafter described.

Figure 2 shows the current application with the post-heat. The current application is comprised of the main welding current application to form a nugget and the post-heat to reform the nugget's microstructure. The main welding current forms the nugget of a predetermined size. Subsequently to the step without current application set for cooling, the post-heat is applied, wherein the current level and the time are varied. The current level of the post-heating is determined based on the main welding current level. Accordingly, the current level ratio (=post-heat current level/main welding current level) becomes one of the key variables. There are three types of post-heat application: the short-time solidification segregation-reducing type, the intermediate-time auto-tempering type and the long-time tempering type. The short-time post-heat type and the intermediate-time post-heat type are hereafter introduced.

In the process of the solidification of molten steel, the density of

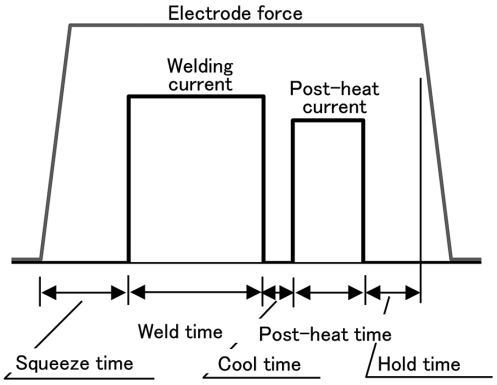

Fig. 2 Spot welding schedule with post-heat by direct current power supply

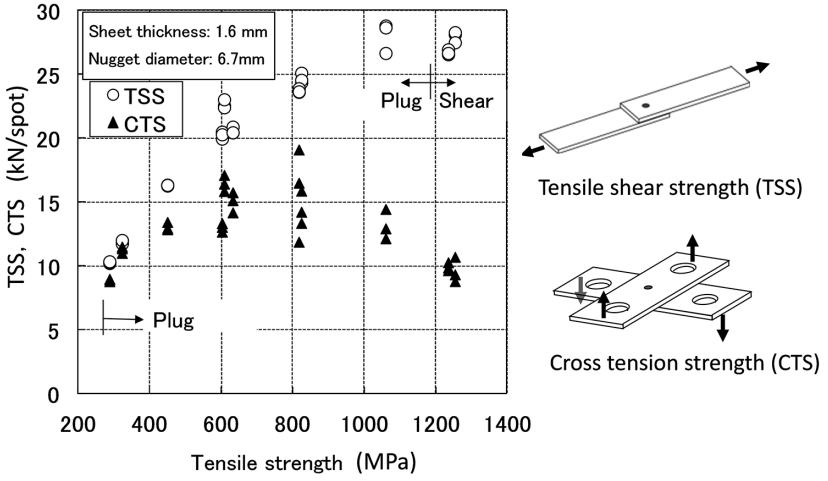

Fig. 1 Effect of base steel strength on TSS and CTS of joints[3]

the solute is higher in the liquid phase than in the solid phase. This phenomenon is the solidification segregation, and the segregation remains in the nugget even when the weld is cooled at room temperature. Particularly, P aggregated locally weakens the interatomic cohesive force and embrittles the steel sheets,[10] and becomes a factor that deteriorates the joint strength in spot welding.[11] In the post-heat segregation-reducing type, the segregated elements are encouraged to disperse by the current applied immediately after the solidification, and the toughness of the nugget is improved thereby.[5] In this type of post-heat , a cooling time of about 0.04–0.12 s is set depending on the sheet thickness (1–2 mm). The cooling step is required to promote the solidification of the molten metal.

Next, a post-heat current of about 90% of the main welding current level was applied for about 0.1–0.2 s. **Figure 3** shows the effect of the post-heat condition on the reduction of the segregation. In the post-heat condition of the 0 s cooling time and the current level ratio of 50%, CTS was not improved, and the strong P contrast is observed at the nugget edge in the image. (The solidification segregation remained.) However, under the post-heat condition of the 0.12 s cooling time and the current level ratio of about 90%, CTS was improved, the P contrast in the image was weak, and the segregation was eliminated. The toughness of the spot weld is improved by this post-heat. As a result thereof, as **Fig. 4** shows, CTS is improved by the post-heat. When the cooling time is increased, with the post-heat current level ratio of 90%, the nugget temperature does not sufficiently rise for the segregated elements to be dispersed. Therefore, the effect of improving CTS is not obtained. Thus, a study is ongoing with respect to the guidelines to determine the segregation-reducing post-heat condition.[12] Additionally, a method of applying the post-heat in a pulsing manner is also under study from the viewpoint of reducing the segregation of elements and improving CTS.[13]

In certain types of steel, the post-heat short-time segregation reducing type does not improve CTS. In such steel types, there are cases in which CTS is improved by increasing the post-heat time. As **Fig. 5** shows, CTS is improved along with the increase of the post-heat time.[14] The cross-sectional view photos above the graph show that the plug diameter (the diameter of the fractured portion of the plug-like shape test piece) increases along with the increase of the post-heat time. **Figure 6** shows the change of the HAZ microstructure along with the change of the post-heat condition. With the

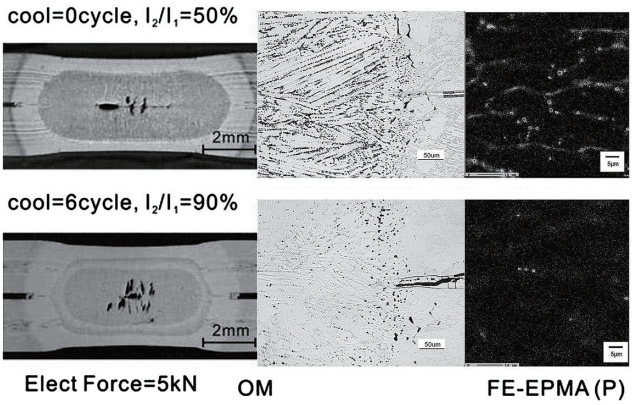

Fig. 3 Effect of post-heat for reduction of solidification segregation on segregation state at nugget edge[5]

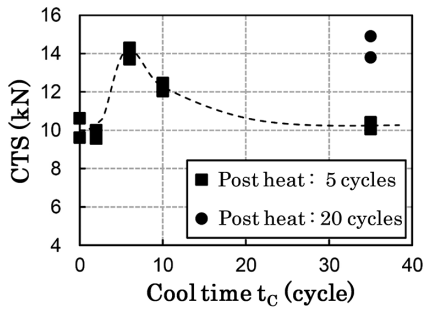

Fig. 4 Effect of cool time in post-heat for reduction of solidification segregation on CTS[5]

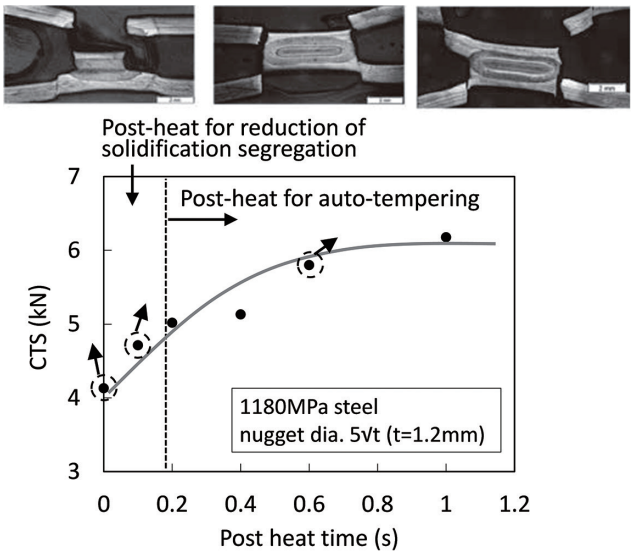

Fig. 5 Effect of time in post-heat for auto-tempering on CTS[14]

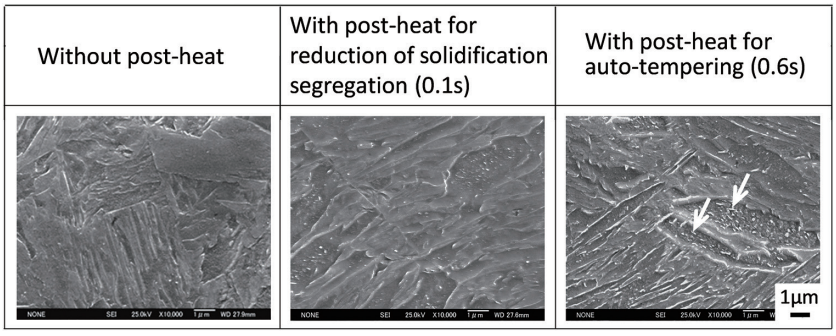

Fig. 6 Change of microstructure at HAZ due to difference post-heat time[14]

0.6 s post-heat, a number of precipitated carbides (shown by arrows in the photograph) are observed. This is the result of the growth by coarsening of the γ grain of HAZ, the raising of the Ms point and the auto-tempering promoted thereby during the cooling of the weld. Thus, in addition to the improvement of the toughness of the nugget, the toughness of HAZ was also improved, as well as CTS.

3. Improvement of Bending Characteristic of Component by Developing the Spot Welding Current Application and Utilization of Arc Spot Welding

Hereinafter, the result of the bending test of the hat-shaped component prepared using a middle carbon high strength steel sheet is described, wherein the weld fracture was suppressed and the absorbed energy of the component was improved. To improve the weld strength of the spot-welded component, enlarging the nugget diameter and the post-heat tempering type were tested. Furthermore, a component was prepared using the AS welding instead of the spot welding, and its effect on suppressing the weld fracture was evaluated.

In this experiment, a 1.4 mm-thick S45C steel sheet containing 0.44 mass% carbon was used. After an austenitizing treatment in a nitrogen atmosphere furnace (retained for 300 s at 1 193 K), the test steel sheet was taken out of the furnace for hardening and for forming into a hat-shaped component as shown in **Fig. 7** by dies. Then it was annealed under the condition for the strength of the component to realize 1 180 MPa grade. The same heat treatments were also applied to a thin rectangular test steel sheet, and this sheet was laid over the flanges of the hat-shaped component, and the overlapped flange portions were spot-welded or AS-welded. For spot welding, the welding conditions for welding the overlapped portions were set so that the diameter of the nugget on the face of the overlapped portions became $3.0\sqrt{t}$ (t: sheet thickness, 3.5 mm) or $5.0\sqrt{t}$ (5.9 mm). The spot welding pitch was 40 mm. In the case of the nugget diameter of $5.0\sqrt{t}$, after a nugget was formed, a post-heat was applied aiming at tempering the nugget. Then the effect of tempering on the energy-absorbing characteristic of the component was evaluated.

For AS welding, a cold metal transfer (CMT) power source was used for the welding machine. In order to obtain stable penetration, prior to the welding, a 4 mm-diameter hole was opened at the weld position on the hat-shaped component flanges. For the welding, a welding wire 1.2 mm in diameter and with a strength grade of 490 MPa was used. The wire feeding speed and the heat input were varied so that the weld metal with different diameters could be formed on the overlapped steel sheets. The welding pitch was 40 mm, the same as that of the spot welding.

Hardness distribution of several cross sections of the welds selected from among the spot-welded welds and the AS-welded welds was measured. The hardness was measured on the top sheet cross section with a measurement load of 9.8 N at a pitch of 0.2 mm at positions 0.2 mm above the overlapping surface. Dynamic three-point bending tests were conducted for the components. The component was placed on two 30 mm-radius supporting rolls arranged 700 mm apart. Then a 50 mm-radius impactor set above the component was collided with the component at a speed of 2 m/s. The load was measured with a load cell installed on the impactor. In this test, the component was placed so that the thin rectangular steel sheet side faces the impactor collision.

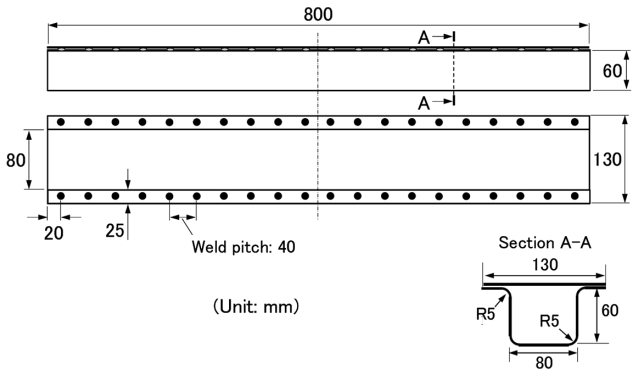

Fig. 7 Schematic of hat-shaped component

Figure 8(a) shows the cross-section view of the spot-welded nugget with a diameter of $5.0\sqrt{t}$. Tempered martensite is observed in the base metal. This microstructure was formed as a result of the above-described quench and temper heat treatment. Martensite was formed in the nugget and HAZ. Figure 8(b) shows the cross-section view of the AS weld metal with a diameter of $5.3\sqrt{t}$. In the case of AS welding, the welding constituted penetration welding, and the excess metal was formed on either the front or back side of the weld. The main phase of the AS weld metal is ferrite, with most of the remaining part occupied by pearlite. The reason for a soft microstructure being formed in the AS weld metal is that the components of the base metal and the welding wire are mixed (for example, carbon content decreases), and the cooling rate of the AS weld is lower than that of the spot weld. In HAZ, ferrite and pearlite are observed in addition to martensite.

In **Fig. 9**, the Vickers hardness distribution of the weld is compared. The nugget Vickers hardness of the spot weld reached HV 700. In the spot weld with a tempering post-heat applied after the

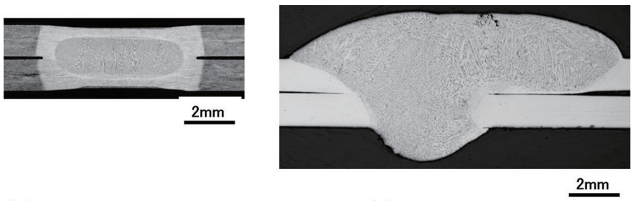

Fig. 8 Cross section of welds

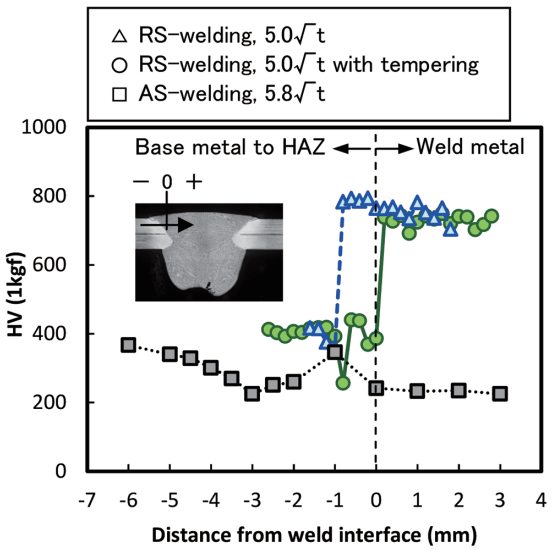

Fig. 9 Distribution of hardness in each weld

formation of the nugget, the hardness at the nugget edge and HAZ decreased to HV400. The AS weld metal hardness is HV250, which is lower than that of the spot weld. Furthermore, the highest hardness of HAZ of the AS weld is similarly lower, which is attributed to the soft microstructure formed as described above.

Figure 10 shows the relationship between the displacement (component push-in quantity) of the impactor and the load obtained from the three-point bending test. In the spot-welded component, the load increases along with the increase of the nugget diameter. Furthermore, the load under the condition of $5.0\sqrt{t}$ with a post-heat for tempering applied is higher than the loads under any other conditions. Figure 10 also shows the relationship between the displacement and the load of the AS-welded component. Throughout the entire displacement range, the load of the AS-welded component is higher than that of the spot-welded components with the nugget diameter of $5.0\sqrt{t}$. Furthermore, in the displacement range below 25 mm, the load of the AS-welded component is higher than that of the spot-welded component with the weld diameter of $5.0\sqrt{t}$ applied with a post-heat for tempering.

The absorbed energy (AE) is herein defined as the load integrated with respect to the displacement within the range of 0–100 mm. **Figure 11** shows the comparisons of the AEs under all conditions. The AEs of both welded components increase along with the increase of the weld diameter. Also, the AE of the spot-welded component with the nugget diameter of $5.0\sqrt{t}$ is improved by 26% as a result of the post-heat for tempering application. When compared under the nearly equal weld metal diameter (spot weld $5.0\sqrt{t}$ and AS-weld $5.3\sqrt{t}$), the AE of the AS-welded component is higher by 26% than that of the spot-welded component. Therefore, it is considered that the AS weld exhibits the same effect as that of the spot weld applied with a post-heat for tempering.

Figure 12 shows the appearances of components after the three-point bending test. In the case of the spot-welded component with the nugget diameter of $3.0\sqrt{t}$, all spot welds were fractured during the bending test. From the observation by a high-speed video camera, the welds fractured at the displacement of 10 mm, and simultaneously, the component was deformed with the wall falling inward. As a result thereof and as shown in Fig. 10, the load decreased beyond the displacement of 10 mm. When the nugget diameter was increased to $5.0\sqrt{t}$, the number of the fractured welds decreased. The weld fracture and the sectional buckling occurred at a displacement larger than the case of $3.0\sqrt{t}$. Furthermore, when the post-heat for tempering was additionally applied to the nugget with a diameter of $5.0\sqrt{t}$, the welds were not fractured during the test. Under such a condition, the hat-shaped component element and the thin rectangular steel sheet restrained the deformation of each other, and the sectional buckling was suppressed. As a result thereof, a load higher than those under any other conditions was maintained throughout the entire range of the displacement.

Also in the case of the AS-welded component with the weld metal with a diameter of $5.8\sqrt{t}$, the weld fracture was suppressed. This is considered to be attributed to the relatively soft weld metal and the excellent toughness of the AS weld that is similar to that of the spot weld with post-heat for tempering applied. As Fig. 8(b) shows, AS-welding formed extra metals. In the early stage of the bending test, the impactor collided head on with the component at the excess metal and at the plurality of locations in the center area. Due to the expanded contact area of the component against the impactor, the load bearing area of the component also expanded, and the sectional buckling in the early stage was suppressed thereby.

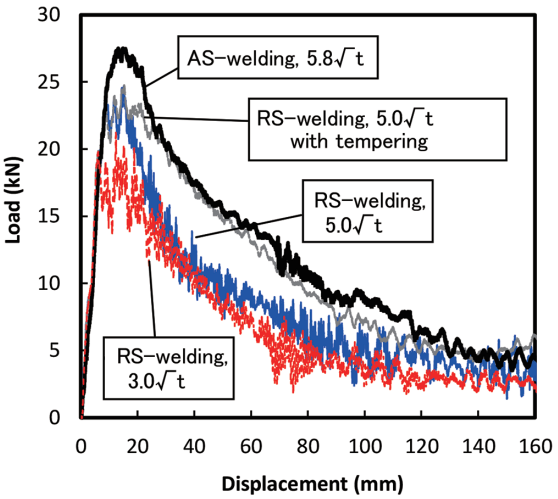

Fig. 10 Load-displacement curves of resistance spot welded or arc-spot welded component obtained in the three-point bending test

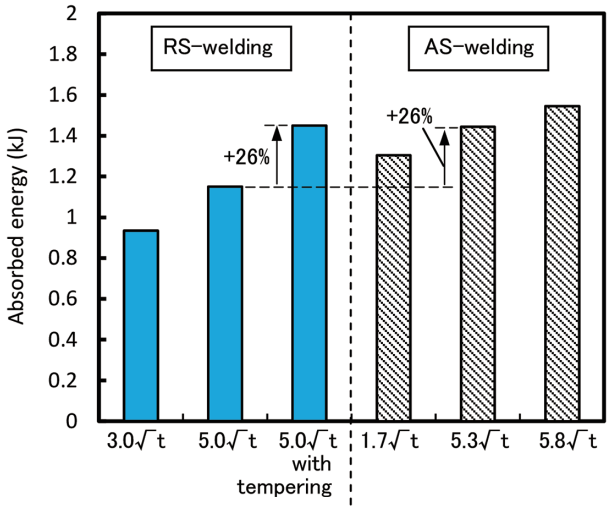

Fig. 11 Comparison of average absorbed energy between resistance spot welded and arc-spot welded components

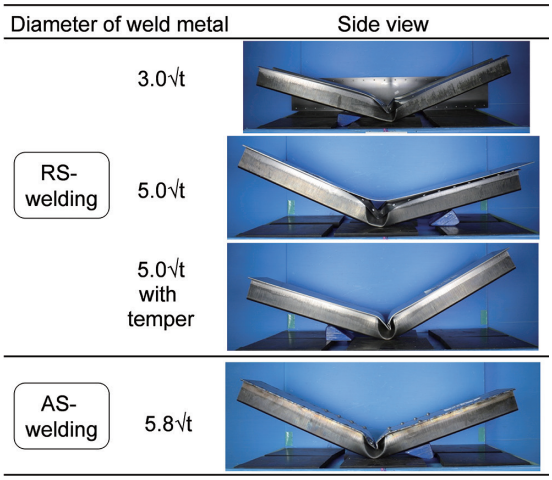

Fig. 12 Appearance of components after the three-point bending test

This "delay in the sectional buckling" is considered to be the reason for the load of the AS weld being higher than that of the tempered spot weld in the range below 25 mm displacement as shown in Fig. 10. However, above the 25 mm displacement range, both loads are almost the same. Accordingly, after the start of the sectional buckling of the component, both have an equal rigidity.

4. Improvement of Component Bending Characteristic with the Combined Use of Spot Welding and Laser Welding

In the high strength hot-stamping steel sheet of 1 500 MPa grade strengthened by transformation to martensite, HAZ is partly tempered and softened by spot welding. Therefore, when a large in-plane tensile load acts upon the spot weld at the collision, stress is concentrated at the softened HAZ area and HAZ is fractured, and sometimes it happens that the required component strength is not secured.[15, 16] To prevent the fracture in the softened HAZ area, the following methods have been reported: softening the peripheral area of the weld prior to spot welding, and designing the component structure so that the strain acting upon the weld is reduced.[16–18] As a method to prevent the fracture with a welding technique, the combined use of the spot welding and the laser welding is reported hereafter.

To evaluate the state of the fracture of the spot weld, a modelled hat-shaped component as shown in **Fig. 13** was prepared by combining a 1 500 MPa grade hot-stamping steel sheet and a 590 MPa grade steel sheet. The length of the component was 300 mm. A hot-stamping thin rectangular steel sheet (50 mm × 22 mm) was spot-welded to the bottom side of the hat-shaped component placed right below the impactor. The weld in this experiment is the subject of the evaluation. Two types of component were prepared: one in which the rectangular steel sheet was joined by spot-welding only, and the other in which the rectangular steel sheet was joined by the spot welding and subsequently by the laser welding applied on the line running over the center of the spot weld. The laser welding was applied in the longitudinal direction of the component (direction of the tensile load), and the length of the laser weld was 40 mm. The spot weld pitch was 50 mm. As **Fig. 14** shows, the component was placed on the two supporting rollers with a radius of 30 mm that were situated 200 mm apart in a position with the 590 MPa grade material side facing the impactor with a radius of 30 mm set directly above it. A static three-point bending test was conducted, wherein the impactor pushed the component downward at a speed of 1 mm/s. During the bending test, the spot weld, the subject of the evaluation, suffered a minor bending deformation in addition to the in-plane tension.

Figure 15 shows the relationship between the displacement of the impactor and the load obtained from the static three-point bending test. **Figure 16** shows the appearance of the component after the test. The component joined with the thin rectangular steel sheet with only spot welding fractured at the displacement of about 22 mm by the strain concentrated at the softened HAZ area. As a result thereof, the collapse of the component section progressed and the load decreased rapidly. On the other hand, in the component joined with the thin rectangular steel sheet with the spot welding and the subsequent laser welding, the spot weld was not fractured, and high load was maintained up to a large displacement. This is because the HAZ area

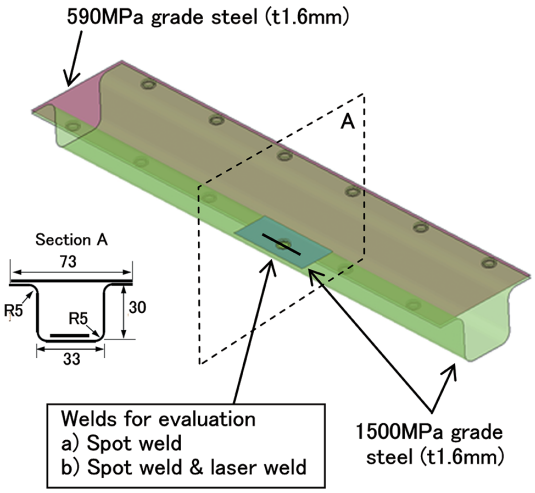

Fig. 13 Schematic of hat-shaped component welded with a small rectangular sheet

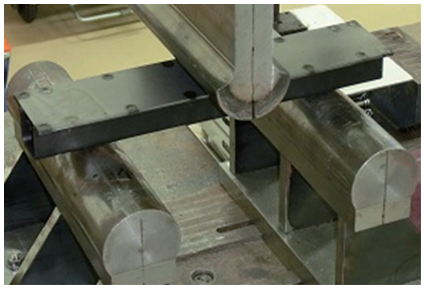

Fig. 14 Setup for three-point bending tests

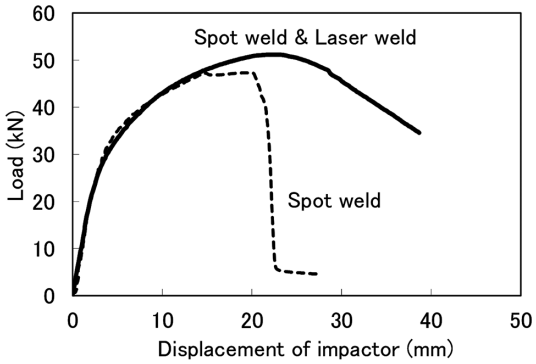

Fig. 15 Load-displacement curves of resistance spot welded component or laser-welded one after resistance spot welding obtained in the three-point bending test

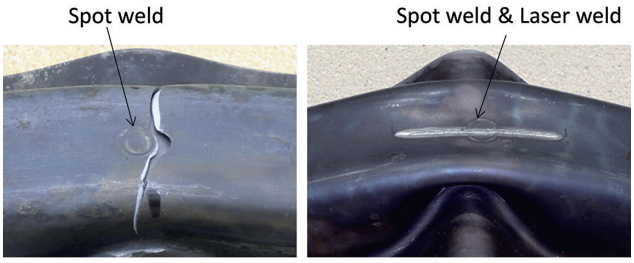

Fig. 16 Appearance of welds after three-point bending test

softened by the spot welding was quenched and hardened again by the laser welding, and the concentration of the strain during bending was suppressed thereby. Thus it was discovered that, by applying the laser welding over the spot weld, the fracture is suppressed and the component performance is significantly improved even when the high stress is imparted by the impactor directly under it.

5. Improvement of Component Bending Characteristic by Ridgeline Joining Welding Patchwork Tailored Blanking Technique Method

To protect the cabin in order to secure the passengers' space in the case of a lateral collision, it is necessary to suppress the deformation of the frame component. The center pillar is typical of such frame component, and a very high bending characteristic is desired. Therefore, high strength steel sheets are used for the center pillar, and furthermore, a reinforcing component element is spot-welded to a part of the center pillar component to establish the desired bending performance. However, with the conventional method, the reinforcing component element is preformed and then built into the preformed center pillar component element. Therefore, as shown in **Fig. 17**(a), a gap is generated between these component elements. With a gap in between, the two component elements are deformed differently at the time of a collision, and misalignment is developed between the two component elements. Namely, the two sheets of the components do not behave as a single sheet, and the effect of improving the bending characteristic by increasing the thickness of the component is not fully exerted. To minimize the gap, the patchwork-tailored welded blanks technique (hereinafter referred to as "PW-TWB") is practically employed.

The perspective view and the cross section view of a component prepared with this method are shown in Fig. 17(b). In this method, the main component element steel sheet and the reinforcing component element steel sheet are joined by spot welding in the flat state and press-formed to the finished component subsequently. With the PW-TWB method, it is also possible to spot-weld the ridge line region (bending R region) of a component before press-forming. The perspective view and the cross section view of a component prepared with this new method are shown in Fig. 17(c). When a bending load is exerted on such a component, the sheets of the component elements at the ridge line region are deformed in a different manner. In the conventional method or in the conventional PW-TWB method, the top sheet and the bottom sheet are deformed differently in the ridge line region as shown in **Fig. 18**(a). Therefore, the effect of the thickened sheet is restrictive. However, in the component wherein the ridge line region is weld-joined with the new PW-TWB method, the ridge line region transmits the stress to the top sheet and the bottom sheet via the weld as shown in Fig. 18(b), and the rigidity of the component was predicted to improve.

Practically, the hat-shaped components as shown in Fig. 17(a)–(c) were prepared, the bending characteristics of which were evaluated. The main component element was: top face width: 80 mm, height: 60 mm, flange width: 25 mm. The reinforcing component element was: top face width: 57.2 mm, height: 40 mm. The closing plate was 140 mm wide, and the length of the component was 600 mm. The steel sheets used for the main component element and the reinforcing component element were the hot-stamping steel sheets of 1 500 MPa grade strength after quenching. The sheet thickness of the main component element was 1.4 mm, and the sheet thickness of the reinforcing component element was 1.2 mm. A 780 MPa grade dual-phase steel with a thickness of 1.8 mm was used for the closing plate. With the conventional technique, the main component element and the reinforcing component element were separately formed by hot-stamping, and subsequently assembled by spot-welding. A 5 mm gap was set between the main component element and the top face of the reinforcing component element.

In the two PW-TWB methods, the blank sheets of the main component element and the reinforcing component element were spot-welded prior to the press-forming, and the two component element blank sheets were hot-stamped under the heating condition of 900°C × 420 s. After press-forming the two component element sheets into a hat-shaped component, the flanges were jointed with the closing plate and a closed section component was structured. The spot weld pitch was 40 mm for all weld-joining of the main component element, the reinforcing component element and the closing plate. Static three-point bending tests (push-in stroke speed: 15 mm/min) were conducted on the thus prepared components, and the stroke vs. load relation was measured. In the bending test, the radii of the two rollers that supported the component were 30 mm, and the rollers were arranged 500 mm apart. The radius of the push-in punch was 150 mm and the maximum push-in displacement was 50 mm.

Figure 19 shows the relationship between the displacement and the load in the three-point bending test. When the maximum loads of the components prepared with the conventional method and those prepared with PW-TWB methods are compared, the latter were im-

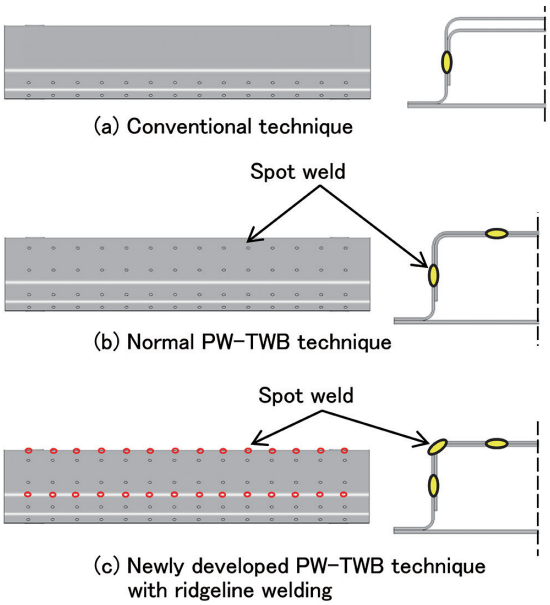

Fig. 17 Comparison of perspective view and cross section of components made by each method

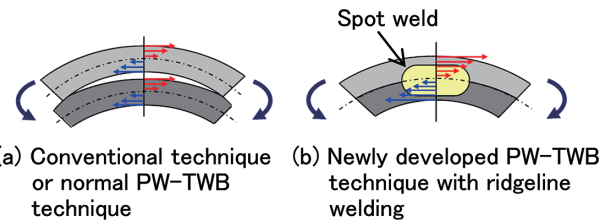

Fig. 18 Comparison of deformation and stress distribution at ridgeline of components subjected to bending

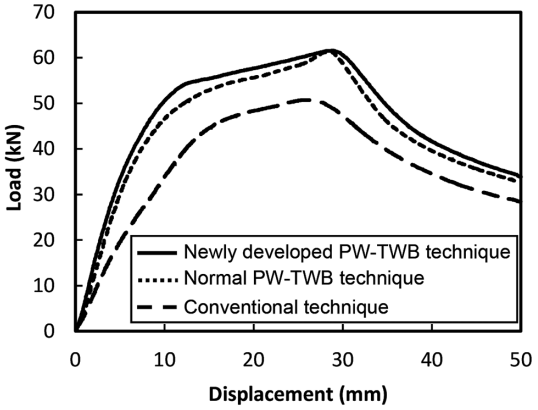

Fig. 19 Load-displacement curves obtained in the three-point bending test for components

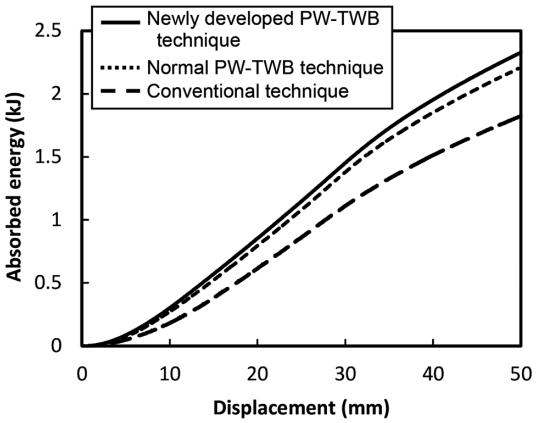

Fig. 20 Absorbed energy-displacement curves obtained in the three-point bending test for components

proved by 22% (50 kN to 61 kN). In **Fig. 20**, the relationship between the displacement and the absorbed energy (AE) is shown. As compared with the AE (at 50 mm displacement) of the hat-shaped component prepared with the conventional method, the AE of the one prepared with the conventional PW-TWB method was improved by 20% (1.8 kJ to 2.2 kJ), and the AE of the one prepared with the new PW-TWB method was improved by 27% (1.8 kJ to 2.3 kJ). Thus, by developing the joining method, the component is able to exert its bending performance in a sophisticated manner. Furthermore, Fig. 20 also suggests that in securing a certain bending performance, the reduction of the thickness of the reinforcing component and the weight reduction of the component thereby are enabled by employing the PW-TWB method.

6. Study on Prevention of LME in Spot Welding (Effect of Enlarging Electrode Tip Front End Diameter)

In the spot welding of the galvanized high strength steel sheet, the liquid metal embrittlement (hereinafter referred to as LME) is generated at the weld in some cases. The LME crack is generated on the surface of the steel sheet subjected to the electrode pressing force applied during the spot welding, or on the overlapped steel sheet surface (near the pressure-welded jointed area).[19] To suppress the crack in the vicinity of the pressure-welded joint area, for instance, prolonging the hold time is effective.[20] The crack is generated by the high tensile stress that is generated at the area when the electrode is released. Simultaneously, the zinc melted by the welding heat is also one of the factors of the cause. It is considered that the molten zinc embrittles the surface layer steel of the sheet. If the hold time is prolonged, once molten zinc is resolidified during the prolonged hold time, the crack is considered to be suppressed thereby. As a method applied to the electrode to suppress the crack, the result of enlarging the electrode tip front end diameter (hereinafter referred to as electrode tip diameter)[21] is described hereunder. At the same time, the result of the study is introduced, which was conducted to determine whether an appropriate current range can be secured even when a gap exists between the sheets as observed in actual components, and even when the electrode tip diameter is enlarged.

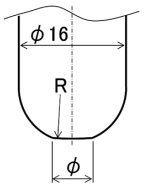

Fig. 21 Schematic of electrode for spot welding

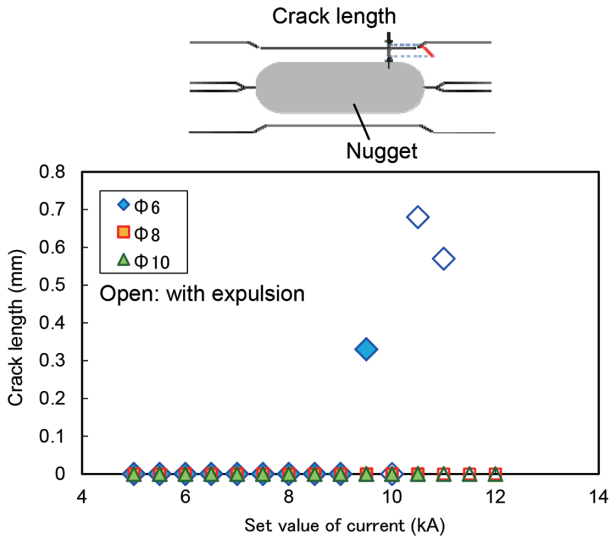

Fig. 22 Relationship between current and LME crack length for each diameter of electrode tip

The sample steel sheet was a 980 MPa grade galvannealed steel sheet (GA) of 1.6 mm thickness. **Figure 21** shows the schematic of the electrode used for the spot-welding. The radius of curvature of the electrode tip front (R) was fixed at 40 mm, and the electrode tip diameter was varied in the range between 6–10 mm. The electrode force, the weld time and the hold time were fixed at 4 kN, 0.4 s and 0.1 s, respectively. The current level was varied. For spot welding, an X type welding gun was used. The X type welding gun triggers an electrode misalignment depending on the welding condition. Therefore, we considered that, in spot welding, the in-plane stress or strain is generated in the steel sheet surface layer contacting the electrode, and the crack is promoted thereby.

Figure 22 shows the relationship between the current level and the LME crack length for the respective electrode tip diameter. In the case of the standard electrode tip diameter of 6 mm, the crack is generated regardless of the occurrence of the spot-welding expul-

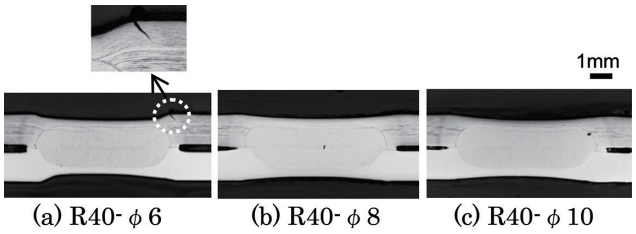

Fig. 23 Suppression of LME cracking through increase of diameter of electrode tip (Nugget diameter: $5\sqrt{t}$)

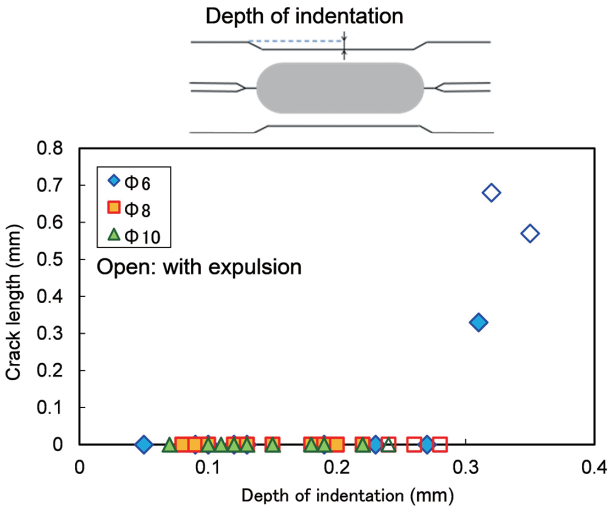

Fig. 24 Relationship between depth of indentation and LME crack length for each diameter of electrode tip

sion in the range above the current level of 9.5 kA. With the electrode tip diameters of 8 mm and 10 mm, the crack was not generated in the entire current level range. In **Fig. 23**, the cross section view of the weld of a nugget with a diameter of $5\sqrt{t}$ (6.3 mm, current level 9.5 kA or 10 kA) is shown as an example. In the case of the electrode tip diameter of 6 mm, a crack was generated outside the indentation (a concave formed on the electrode side steel sheet surface) as shown by a broken line circle. However, in the cases of the electrode tip diameters of 8 mm and 10 mm, cracks were not generated. By referring to Fig. 23, the depth of the indentation (ID) differs depending on the electrode tip diameter. ID tends to increase as the current level and the nugget diameter increase.

Next, in **Fig. 24**, the crack length generated under various conditions is arranged with respect to ID and shown. The figure shows that, with the electrode tip diameter of 6 mm, a crack is generated when ID is above 0.3 mm. With the electrode tip diameter of 8 mm or above, cracks are not generated at any IDs. Even in the case of the electrode tip diameter of 8 mm or above, ID is controlled to below 0.3 mm even under the spot-welding expulsion condition. Accordingly, the reason for the enlarged electrode tip diameter suppressing the crack is considered to be attributed to the reduction of the stress and the strain at the steel sheet surface realized by the reduction of ID. Furthermore, the reduction of ID is considered to be attributed to the reduction of the current density, the promotion of the electrode cooling (suppression of the steel sheet surface temperature rise) and the reduced unit surface pressure, all realized by enlarging the electrode tip diameter. Additionally, it is also reported that the increase of the electrode tip front curvature is similarly effective in suppressing the crack at the surface layer of the steel sheet

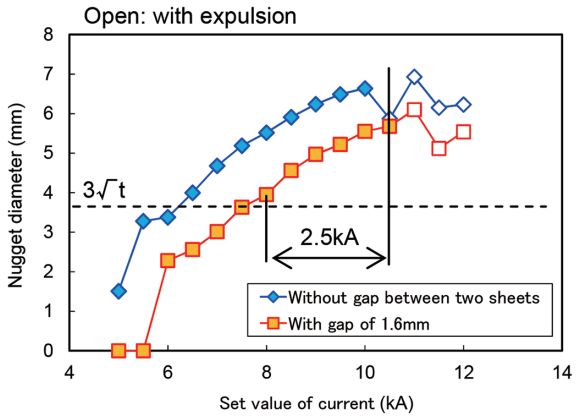

Fig. 25 Comparison of appropriate current range in welding without gap between two sheets and with that of 1.6 mm (Electrode tip diameter: 13 mm)

contacting the electrode.

Furthermore, an appropriate current range was examined for the case of a gap existing between the steel sheets. The gap between the steel sheets was set at 1.6 mm, and the electrode tip diameter was set at 6 mm and 13 mm, respectively. In this study, a 1.6 mm thickness test steel sheet of the 980 MPa grade galvannealed (GA) steel sheet was used. **Figure 25** shows the relationship between the current level and the nugget diameter in the case of the electrode tip diameter of 13 mm. The appropriate current range applicable to both cases of with and without the gap (from the current level that forms the nugget with a diameter of $3\sqrt{t}$ up to the current level where the spot-welding expulsion starts to occur) is 2.5 kA (8–10.5 kA), the range of which is considered to be sufficient for commercial production. Under the condition of the electrode tip diameter of 6 mm tested for comparison, the appropriate current range applicable to both cases of with and without the gap is 2.5 kA. As far as this study is concerned, it is thus concluded that even if the electrode tip diameter is enlarged, the appropriate current level range does not change.

7. Development of Dissimilar Material Joining Technique by Utilizing EJOWELD®

The employment of dissimilar materials is also a means to reduce the car body weight. Namely, various materials such as steel, aluminum and plastic can be appropriately applied to car bodies, and upon assembling car bodies, an appropriate joining method is selected depending on the combination of such materials. In the joining of steel and aluminum, for instance, the mechanical joining method represented by the self-piercing rivet is the mainstream method. For instance, the EJOWELD® developed by EJOT is employed for joining aluminum and the 1 500 MPa grade hot-stamping steel sheet. Nippon Steel Corporation is also developing the steel and aluminum sheet joining technique by using EJOWELD®. In **Fig. 26**, the cross section view of the weld joint obtained by EJOWELD® is shown. In this joining method, the rivet-like piece called an “element” firstly penetrates the top aluminum sheet by the rotation and the pressurization imparted. The element and the bottom steel sheet are friction-pressure joined, and in order to achieve joining, the element head presses the top sheet simultaneously.

As an example of the study, a CTS test piece of the combination of the alloy aluminum (A6061) top sheet and the 590–1 500 MPa grade cold rolled steel bottom sheet was prepared, and the joint strength was evaluated. The thickness of both sheets was 1.6 mm.

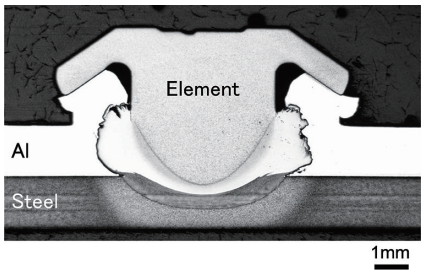

Fig. 26 Cross section of weld made by EJOWELD®

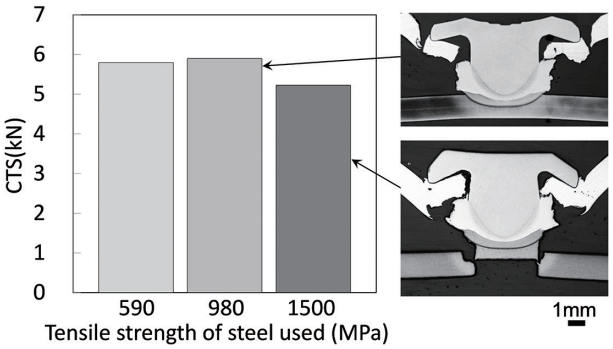

Fig. 27 Comparison of CTS of EJOWELD® joints made by combining aluminum and steels with various strengths

Figure 27 shows the cross tensile strength (CTS) of the respective joint and the cross section view of the weld joint part after fracture. In the CTS test with the combination of the alloy aluminum sheet and the 590 MPa or the 980 MPa grade steel, the top alloy aluminum sheet was fractured. Accordingly, the strength of the friction-pressure-joined joint of the element and the steel sheet is higher than that of the aluminum sheet. However, under this joining condition, in the cross tensile test with the combination of the alloy aluminum sheet and the 1 500 MPa grade steel, the bottom sheet was fractured in the thickness direction. CTS deteriorated slightly as compared with other steels. Hereafter, we are determined to make efforts to determine the conditions that enable the improvement of the joint strength in the combination of aluminum and ultrahigh strength steel sheets, and wish to contribute to the weight reduction of car bodies by the application thereof.

8. Conclusion

Hereafter, further strong compatibility of high strength and high ductility is considered to be required for automotive steel sheets. Nippon Steel continues to tackle the development of such advanced high strength steel sheets, and to propose the techniques to use such steel sheets effectively. Among them, securing the high reliability of the weld strength is crucial to expanding its application. Therefore, this report described the examples of the study targeted at improving the weld strength. It is our great pleasure to find that such development constitutes a part of the base that supports the development of the automotive industry.

References

1) Sato, A.: Problem of High Strength Steel Sheet and its Countermeasures. Journal of the JSTP. 46 (534), 548–551 (2005)
2) Clare, G.: Welding Advanced High-strength Steel is Pushing Welding Technology. Penton's Weld Mag. 81 (3), 14–16, 18 (2008)
3) Oikawa, H. et al.: Spot-weld Weldability of High Strength Steel Sheet for Automotive Use. Shinnittetsu Giho. (385), 36–41 (2006)
4) Herai, T., Takahashi, Y.: Resistance Spot Welding of High Strength Steel Sheets. IIW Doc. III-612-79, 1979
5) Hamatani, H. et al.: Cross Tensile Strength Property of High Strength Steel Sheet Spot-welded Joint. Preprints of the National Meeting of JWS. 89, 44–45 (2011)
6) Furusako, S. et al.: Strength of Arc Spot Welded Joints in a High Strength Steel Sheet. SAE 2014 World Congress, Material, 2014-01-0786
7) Furusako, S. et al.: Fatigue Strength of Arc Spot Welded High Strength Steel Joint (First Report). Preprints of the National Meeting of JWS. 96, 114–115 (2015)
8) Yamazaki, K. et al.: Strength Property of Spot-welded Joint of Ultra High Strength Cold Rolled Steel Sheet. Transactions of JWS. 17 (4), 553 (1999)
9) Watanabe, F., Furusako, S., Hamatani, H., Miyazaki, Y., Nose, T.: Fracture Mechanical Analysis of Cross Tension Test for High-Strength Steel Spot Welded Joints. Mathematical Modeling of Weld Phenomena. 10, 653 (2012)
10) Yamaguchi, M.: First Principle Calculation of Grain Boundary Cohesive Energy: Segregation of Solute Element and Embrittlement at bcc Fe Σ3(111) Grain Boundary and Strengthening Effect. J. Jpn. Inst. Met. 72 (9), 657–666 (2008)
11) Furusako, S. et al.: Effect of Added Elements on Spot-welded L-type Joint Strength and Fracture Behavior. Transactions of JWS. 33 (2), 133–143 (2015)
12) Furusako, S. et al.: Study on Guide Line for Determining Spot-welding Conditions by Using Heat Conduction Analysis Solution. Transactions of JWS. 33 (2), 160–170 (2015)
13) Taniguchi, K. et al.: Development of Pulse Energization Spot-welding Technique for High Strength Steel Sheet (Third Report). Preprints of the National Meeting of JWS. 90, 240–241 (2012)
14) Wakabayashi, C. et al.: Improvement of Spot-welded Joint Strength by Promoting Auto-tempering of HAZ. Preprints of the National Meeting of JWS. 96, 38–39 (2015)
15) Fujimoto, H. et al.: Effect of Softening of HAZ on Stress and Strain in In-plane Tensile Strength Test of High Strength Steel Sheet Spot-welded Joint. Preprints of the National Meeting of JWS. 34 (4), 285–294 (2016)
16) Fermer, M. et al.: Local Annealing of Hot-formed Steel for Improved Ductility and Spot Weld Strength. Proceedings of Material in Car Body Engineering 2012. Bad Nauheim, p.1–22
17) Nakamura, T. et al.: Development of Light Weight Body Shell for New Type MAZDA AXELA. Mazda Technical Review. 31, 14–18 (2013)
18) Hirose, S. et al.: Study on the Countermeasures for Weld Fracture of Spot-weld of the Car Body Frame of Ultrahigh Strength Steel Sheet (Fourth Report)—Study on Prevention of Fracture in HAZ in the Periphery of Spot weld. Preprints of Society of Automotive Engineers of Japan, Inc. 2018 Spring Meeting Scientific Lecture. 20185206, 1–4 (2018)
19) Choi, D.Y. et al.: Parametric Study for Liquid Metal Embrittlement in Resistance Spot Welds of Galvanized TRIP Steel. Sheet Metal Welding Conference XVIII. October 17–18, 2018
20) EuroCarBody 2018: Nissan Infiniti QX50
21) Sierlinger, R., Gruber, M.: A Practical Approach to Evaluate the Susceptibility of Zinc Coated Steels to Liquid Metal Embrittlement (LME) during Spot Welding. Joining in Car Body Engineering 2017, April 2017

Seiji FURUSAKO
Senior Researcher, Dr.Eng.
Welding & Joining Research Lab.
Steel Research Laboratories
20-1 Shintomi, Futtsu City, Chiba Pref. 293-8511

Sho MATSUI
Welding & Joining Research Lab.
Steel Research Laboratories

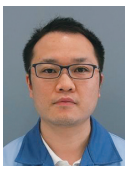

Tasuku ZENIYA
Researcher
Integrated Steel-Solution Research Lab.
Steel Research Laboratories

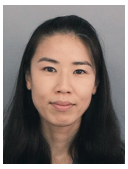

Chisato WAKABAYASHI
Senior Researcher, Dr.Eng.
Welding & Joining Research Lab.
Steel Research Laboratories

Tohru OKADA
Senior Researcher
Welding & Joining Research Lab.
Steel Research Laboratories

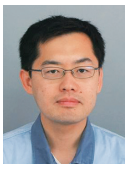

Naoaki SHIMADA
Senior Researcher
Welding & Joining Research Lab.
Steel Research Laboratories

Hiroki FUJIMOTO
Senior Researcher, Dr.Eng.
Welding & Joining Research Lab.
Steel Research Laboratories